



Published in final edited form as:

J Shoulder Elbow Surg. 2013 December ; 22(12): . doi:10.1016/j.jse.2013.03.014.

Evaluation of cartilage degeneration in a rat model of rotator cuff tear arthropathy

Erik J. Kramer, BA^{1,2,*}, Blake M. Bodendorfer, BS^{1,*}, Dominique Laron, MD², Jason Wong, BA¹, Hubert T. Kim, MD^{1,2}, Xuhui Liu, MD^{1,2}, and Brian T. Feeley, MD²

¹Department of Veterans Affairs, San Francisco Veterans Affairs Medical Center, San Francisco, CA, USA

²Department of Orthopaedic Surgery, University of California, San Francisco, CA, USA

Abstract

Introduction—Rotator cuff tears are the most common injury seen by shoulder surgeons. Many late stage rotator cuff tear patients develop glenohumeral osteoarthritis as a result of torn cuff tendons, termed cuff tear arthropathy. However, the mechanisms of cuff tear arthropathy have not been fully established. It has been hypothesized that a combination of synovial and mechanical factors contribute equally to the development of cuff tear arthropathy. The goal of this study was to assess the utility of this model in investigating cuff-tear arthropathy.

Methods—We utilized a rat model which accurately reflects rotator cuff muscle degradation after massive rotator cuff tears through either infraspinatus and supraspinatus tenotomy or suprascapular nerve transection. Using a Modified-Mankin Scoring System (MMS), we found significant glenohumeral cartilage damage following both rotator cuff tenotomy and suprascapular nerve transection after only 12 weeks.

Results—Cartilage degeneration was similar between groups, and was present on both the humeral head and the glenoid. Denervation of the supraspinatus and infraspinatus muscles without opening the joint capsule caused cartilage degeneration similar to that found in the tendon transection group.

Conclusions—These results suggest that altered mechanical loading after rotator cuff tears is the primary factor in cartilage degeneration after rotator cuff tears. Clinically, understanding the process of cartilage degeneration after rotator cuff injury will help guide treatment decisions in the setting of rotator cuff tears.

Level of evidence—Basic Science Study, Animal Model

© 2013 Journal of Shoulder and Elbow Surgery Board of Trustees. Published by Mosby, Inc. All rights reserved.

Corresponding Author: Brian T. Feeley, MD, Sports Medicine and Shoulder Surgery, Department of Orthopaedic Surgery, 1500 Owens Ave, Box 3004, San Francisco, CA 94158, USA, feeleyb@orthosurg.ucsf.edu.

*Both authors contributed equally to this work

Conflicts of Interest:

No authors have any conflicts of interest to disclose.

Study Approval: All animal procedures were approved by our IACUC (A3476-01). The histologic pictures should be published in color.

Publisher's Disclaimer: This is a PDF file of an unedited manuscript that has been accepted for publication. As a service to our customers we are providing this early version of the manuscript. The manuscript will undergo copyediting, typesetting, and review of the resulting proof before it is published in its final citable form. Please note that during the production process errors may be discovered which could affect the content, and all legal disclaimers that apply to the journal pertain.

Keywords

massive rotator cuff tear; arthropathy; osteoarthritis; histology; articular cartilage

Introduction

The rotator cuff acts as the primary dynamic stabilizer of the glenohumeral joint, initiates shoulder motion, controls joint position, and depresses the humeral head with shoulder abduction and forward flexion. In the setting of small and medium sized cuff tears where force couples in between the subscapularis and infraspinatus are maintained, there is normal glenohumeral motion and in most cases, no evidence of degenerative changes within the cartilage. With large and massive tears, normal glenohumeral motion is theoretically possible, but the combination of pain and loss of the supraspinatus-deltoid and supraspinatus-subscapularis force couples lead to abnormal joint kinematics and motion patterns, and ultimately to cartilage wear and deterioration of shoulder function. This phenomenon was originally described by Neer et al as cuff tear arthropathy.^{4; 9} In addition to abnormal loading, Neer also postulated that synovial fluid loss decreases delivery of nutritional factors to the joint, contributing to the degeneration of cartilage and deterioration of shoulder function.

There is currently only limited data evaluating the pathophysiology of articular cartilage changes in the development of cuff tear arthropathy. Reuther et al have observed decreased cartilage thickness in the glenohumeral joints of rats using ultrasonography in a small animal model of massive rotator cuff tears.¹² However, no investigators have used histological methods to assess the degenerative changes in the articular cartilages in a similar model. We previously published a rat model for massive rotator cuff tears in which we observed severe muscle atrophy and fatty degeneration in the supraspinatus and infraspinatus following delivery of complete tendon transection or denervation.⁷ In this study, we utilized our model to assess the effects that tendon transection and denervation have on glenoid and humeral head cartilage. A Modified Mankin scoring system was used to evaluate cartilage health. Current literature suggests that tendon transection would cause abnormal joint mechanics and loss of nutritional factors, while denervation would only cause abnormal joint mechanics and therefore less damage to the glenohumeral cartilages. Thus, we hypothesized that (I) tendon transection would lead to a significant increase in histologic cartilage injury as assessed by Mankin score; and (II) denervation would lead to a comparatively smaller increase in histologic cartilage injury.

Materials and Methods

Ten 3-month-old female Sprague–Dawley rats (Charles River Laboratories, Inc., Wilmington, MA, USA) at 250 g weight were randomly divided into two groups: (1) tendon transection only (TT); and (2) suprascapular nerve transection (DN), as described in our past study.⁷ The contralateral limb for each animal received a sham control surgery. The animals were sacrificed twelve weeks postoperatively and both shoulders were harvested. The Institutional Animal Care and Use Committee approved the experimental design and all surgical procedures in this study.

Surgical Procedure

Animals underwent general anesthesia using 2% isoflurane with oxygen. In the tendon transection group, skin covering the glenohumeral joint was opened, and a longitudinal incision was made through the deltoid to allow access to the rotator cuff tendons at the humeral head, leaving the biceps intact. The supraspinatus and infraspinatus tendons were

cut at their insertion into humeral head. In the denervation group, the trapezoid was incised and the suprascapular nerve root was sharply transected. The shoulder joint capsule was kept intact. The deltoid and/or trapezius muscle were closed with 6-0 prolene sutures and the skin with 5-0 prolene sutures. To establish intra-animal controls, a sham surgery was applied to the contralateral limb: the shoulder was opened, and the respective incision(s) were performed without transecting either the tendons or the nerve, and closed similarly. Animals were resuscitated under a heat lamp and housed in normal conditions.

Glenohumeral Joint Harvest and Decalcification

Animals were sacrificed twelve weeks after surgery. Surgical and sham side front limbs were amputated at the clavicle and removed from the body. Both the clavicle and humerus were bisected and discarded, saving only the glenohumeral joint and the surrounding tissues. The samples were decalcified using a 10% (w/v) ethylenediaminetetraacetic acid (EDTA) (Acros, NJ, USA) with 2.42% (w/v) tris-hydroxymethyl-aminomethane (Tris Base) (Fischer Scientific, Inc., Fair Lawn, NJ, USA), at pH = 8.0 for two months. The decalcifying solution was renewed twice a week.

Paraffin Sectioning

Upon complete decalcification, the glenohumeral joints were dehydrated and the anterior aspect of the joints were embedded face down in a neutral position in paraffin. Sectioning proceeded on the coronal plane. Seven micron-thick sections were taken and mounted on slides for histological analysis.

Safranin-O Staining and Modified Mankin Score Evaluation

Slides were stained with safranin-O in conjunction with hematoxylin and fast green counterstains to visualize proteoglycan content. Samples were stained using 80% hematoxylin (Fischer Scientific, Inc.), and quickly dipped in 1% ammonia water. Next, they were stained using a 0.02% (w/v) Fast Green solution (Sigma-Aldrich, St. Louis, MO, USA). Finally, a 0.1% (w/v) safranin-O (Fischer Scientific, Inc.) stain was applied. Modified Mankin Scores (MMS) for histological evaluation of osteoarthritis are widely used scales (Table I). The numerical outputs are based on qualitative assessments of cartilage morphology, cell distribution, safranin-O staining, and tidemark integrity (Figure 1).^{8, 14} Only coronal sections that included the long biceps tendinous origin were selected for our scoring. In our analyses, we introduced regional specificity by defining three discrete regions of both the humerus and glenoid cartilage; superior, middle, or inferior. Regions were selected by dividing the arc of humerus or glenoid cartilage into thirds (Figure 1). Two independent observers (B.M.B., E.J.K.) blinded to treatment group performed the scoring. Total scores were averaged by cartilage type (humerus or glenoid), region (superior, middle, or inferior), and group (tendon transection or denervation).

Statistical Methods

An a priori power analysis was performed to determine the number of the number of animals needed between groups. Using a difference in MMS of 2 points, with an alpha of 0.05 and a beta of 0.80, 4 animals were needed in each group. An interclass correlation was performed in order to determine agreement between observers in the MMS. Mann-Whitney U tests determined if significant differences existed among surgical and sham sides within TT and DN groups. Kruskal-Wallis tests were also used to determine if significant differences existed among regions. Significance was determined as a p value <0.05. Data is presented as the mean +/- SD.

Results

All animals tolerated the surgery well and survived for 12 weeks with no complications. In evaluation of the cartilage changes in the control sides of both the tendon transection and denervation groups, there were no significant differences in any of the subregions on the glenoid or humeral side. The interclass correlation was 0.84.

Humeral Head

There were significant cartilage changes on the humeral head following tendon transection compared to the control side. The average Modified Mankin Score (MMS) was 1.96 \pm 0.97 in the control group and 5.67 \pm 1.85 in the tendon transection group ($p < 0.001$). In subregion analysis of the humeral head, the MMS was significantly higher in all 3 quadrants in both the tendon transection and denervation groups compared to controls (Table II). Histologic evaluation of the tendon transection group demonstrated relatively consistent degeneration. Structurally, samples in the rotator cuff tenotomy group displayed surface irregularities and development of pannus, while clefts in the cartilage were not often observed. Samples in the tendon transection group also displayed cloning, as well as moderate hypocellularity. All showed decreased proteoglycan content (loss of safranin-O dye) and tidemarks crossed by blood vessels (Figures 2, 3).

Denervation also caused similar damage to the humeral head, where the average MMS was 1.58 \pm 1.36 in the control group compared to 6.17 \pm 1.08 in the denervation group ($P < 0.001$, vs. control; $p = 0.13$ vs. TT). Subregion analysis showed that MMS was significantly higher in all 3 quadrants in the denervation group compared to controls (Table II). Histologic evaluation of the humeral head in the DN group often showed surface irregularities seen in the tendon transection group. However, the development of pannus was less frequent in the denervation group. No clefts were observed. Cloning also was less frequent in the denervation group compared to the tendon transection group, though diffuse hypercellularity was often present. Similar to the tendon transection group, every sample in the denervation group showed loss of proteoglycan content and tidemarks crossed by blood vessels.

Glenoid

The degenerative changes observed in the humeral head also occurred on the glenoid following tendon transection (Figure 4). The average MMS was 2.41 \pm 0.78 in the control group and 5.13 \pm 1.87 in the tendon transection group ($p < 0.001$). Subregion analysis of the glenoid following tendon transection revealed that MMS was significantly higher in all 3 quadrants compared to controls (Table III). Qualitative trends observed in the glenoid were identical to those found in the humeral head following tendon transection.

Denervation caused similar changes to both the humeral head and the glenoid. In the glenoid, the average MMS was 3.22 \pm 1.35 in the control group and 6.33 \pm 0.75 in the denervation group ($p < 0.001$ vs. control; $p = 0.09$ vs TT). Subregion analysis of the glenoid following denervation revealed that MMS was significantly higher in all 3 quadrants compared to controls (Table III). Qualitative trends observed in the humeral head were identical to those found in the glenoid following denervation.

Aggregate Cartilage Scores

MMS for each parameter were aggregated for each region of both the tendon transection and denervation groups (Figure 5). There was no significant difference between sham side shoulders of the tendon transection and denervation groups in either the superior, middle, or inferior regions of both the humerus and glenoid. Differences between sham and surgical

tendon transection samples were significant among all regions with average global scores at 2.42 \pm 1.31 for sham and 6.40 \pm 1.4 for surgery ($p < 0.01$). Differences between sham and denervation samples were also significant among all regions with average global scores at 2.11 \pm 1.2 for sham and 6.0 \pm 1.5 for surgery ($p < 0.01$). Comparison between the tendon transection and denervation groups revealed no significant difference in either the superior, middle, or inferior regions of both humerus and glenoid. Overall, scores were slightly higher in the inferior region of both humerus and glenoid in surgical samples, but not significantly so.

Discussion

In this study we evaluated the development of cuff tear arthropathy in a rat model of massive rotator cuff tears. This is the first study to characterize the rat humeral cartilage changes in a rotator cuff model. We found that creation of a massive rotator cuff tear with transection of the rotator cuff tendons resulted in cartilage degeneration on both the humeral head and glenoid. Interestingly, we also found that denervation produced a similar pattern of degeneration, contrary to our second hypothesis.

Neer et al. hypothesized that cuff tear arthropathy is caused by a combination of abnormal joint loading and loss of nutritional factors via extravasation of synovial fluid.⁹ In this study, we created two different forms of injury to the glenohumeral cartilage. In the tendon transection group, we transect the supra- and infraspinatus tendons which leads to both altered mechanical loading on the glenohumeral joint and loss of nutritional factors containing synovial fluid from the glenohumeral joint. In the denervation group, altered mechanical loading on the glenohumeral joint is achieved by the denervation-induced unloading of supraspinatus and infraspinatus muscle. However, the nutritional factors containing synovial fluid are preserved because the joint capsule remains intact. By comparing the glenohumeral cartilage damage in both groups, we can evaluate the differential effects of nutritional factor loss and mechanical load alterations in cuff tear arthropathy.

In humans, imbalance in stabilizing joint forces caused by rotator cuff tear leads to anterosuperior migration of the humeral head, creating abnormal joint mechanics. The compromised rotator cuff is counteracted by the deltoid, causing migration of the humeral head. Oh et al¹⁰ identified that critical tear sizes causing disrupted joint kinematics are those with full-thickness supraspinatus tears and 50% detachment of the infraspinatus. At maximum internal rotation and all angles of abduction, their cadaveric model showed that these tears led to posterior shifts as large as 3.2 mm. Larger tears, those with both supraspinatus and infraspinatus fully detached, led to posterior shifts as large as 3.5 mm at maximum internal rotation, and superior shifts as large as 2.0 mm at 0° of rotation. In our model, the tendon transection group received what would be equivalent to a massive rotator cuff tear. The anterosuperior migration that Oh et al demonstrated provides a mechanistic explanation to the marked degeneration we observed in both glenoid and humerus cartilage. However, biomechanical loading seems to be dissimilar between human rotator cuffs and those in rats, which could explain why we observed a global degeneration versus a localized degeneration, as seen in humans.

One of the most interesting findings in this study was that, degradation was visualized only 12 weeks suggesting, that loss of the force couple effect can quickly affect the health of the glenohumeral cartilage. Using a similar rat model, Reuther et al¹² investigated changes in glenoid cartilage thickness and mechanical properties using ultrasonography. This elegant study utilized ultrasound and indentation to evaluate cartilage thickness and mechanical properties. It showed widespread thinning of the glenoid, with the most prominent

degeneration and loss of mechanical properties occurring in the anteroinferior portions after only 4 weeks. Our studies showed agreement in that both found the most degeneration in the inferior portions of the glenoid. However, our study used a coronal plane to examine the cartilage, and we were unable to observe statistically significant differences between the anterior and posterior halves of the glenoid. We expanded on this study to show that cartilage changes are also found on the humeral head. Taken together, these studies have important clinical relevance as they show early cartilage degeneration when there is a loss of the mechanical properties of the joint. Clinically, this suggests an additional rationale to repair larger rotator cuff tears in order to decrease the risk of early cartilage degeneration.

Neer et al postulated that loss of the synovial fluid led to degeneration of cartilage through loss of trophic factors and joint lubrication⁶. Thus, it was expected that denervation of the rotator cuff would not lead to as much articular cartilage degeneration as the tendon transection group due to the fact that the joint capsule remained intact and thus the cartilage would continue to receive nutrients from the synovial fluid. However, the amount of cartilage degeneration was similar between groups, suggesting that aberrant mechanical forces are the primary cause of articular cartilage degeneration in the setting of cuff tear arthropathy. Few studies since Neer's 1983 hypothesis have explored the direct role of synovial fluid and glenohumeral joint health.^{5; 16} It is now known however, that the concentrations of cytokines and catabolic enzymes is dramatically increased in the early stages of osteoarthritis. Several studies have shown that rotator cuff tears lead to increased production of IL-1 and TNF- α , which lead to pain and inflammation. It has also been shown that the production of several cartilage-matrix specific MMPs is increased, including MMP-1, MMP-2, MMP-3, MMP-8 and MMP-13.^{3; 11} The presence of MMP-3 is significant, as it is implicated in the proteolytic activation of the other MMPs. One study, by Yoshihara et al has shown that there is indeed a correlation between the concentration of these cytokines, collagenases and aggrecanases and accelerated cartilage degeneration following a cuff tear.¹⁷ These findings implicitly contradict Neer's hypothesis that loss of synovial fluid contributes to the pathogenesis of cuff-tear arthropathy, in that partial synovial fluid evacuation of the joint space may actually be beneficial to cartilage health. More research is needed to fully understand the relationship between nutrient retention versus cytokine and collagenase loss, and to determine the concentration thresholds at which these synovial factors are either beneficial or detrimental. Although we did not directly measure synovial fluid factors, the fact that both groups had equal cartilage degeneration suggest that abnormal mechanics have a primary role in the development of cartilage degeneration in the shoulder.

This study has some limitations. First, the MMS as adopted in this study, relies on the experience of the observers. Like other histological scoring systems, variations between reviewers are sometimes significant. In our study, both of our blinded observers were trained by a single orthopaedic surgeon (B.T.F.) in order to reduce the variation. As a consequence, scores from both reviewers are very similar in each sample. Our interclass correlation was 0.84, and therefore, we believe our results are reliable. Second, we did not evaluate the osseous degradation change of subchondral bone in the glenohumeral joint in this study with radiographic or histologic methods. Thus, the histological pathology of cuff tear arthropathy cannot be compared to radiological findings. Studies suggest that there are changes in the subchondral bone associated with early cartilage degeneration.^{1; 6; 13} Future studies may examine these changes using high resolution imaging modalities such as micro-CT scanning. Third, only one time point was evaluated in this study. It is possible that the rate of cartilaginous degeneration differed between the tenotomy and denervation group, with one presenting a more acute progression profile, while the other may be more chronic in nature. A future study is needed to explore this possibility. Finally, while it has been

established that rats have similar shoulder morphologies to humans, they are quadrupeds and thus have dissimilar joint loading mechanics.^{2; 15}

Conclusions

In conclusion, this study confirmed that our rat model is feasible for histopathologic evaluation of cartilaginous degeneration following massive rotator cuff tears. Our histopathological results demonstrated similar severity of cartilage breakdown after both tendon transection and denervation. Because the joint capsule was intact in the denervation procedure, it is unlikely the nutrient factors in the joint fluid were lost in the denervated joint. Thus, altered biomechanical loading in the glenohumeral joint surface, rather than the loss of joint fluid plays a critical role in glenohumeral cartilage damage following rotator cuff tears. Furthermore, recent studies have found a positive correlation between the concentration of cytokines and catabolic enzymes and the rate of arthropathic progression, suggesting that the presence of synovial fluid may actually be detrimental to articular health following a rotator cuff tear. This model can be used to better understand cartilage degeneration in the shoulder and to evaluate the effects of treatment modalities on preventing cartilage injury in the setting of rotator cuff tears.

Acknowledgments

Source of Funding:

Funding was provided from a grant from the OREF (Young Investigator Grant)

References

1. Chou CH, Lee CH, Lu LS, Song IW, Chuang HP, Kuo SY, et al. Direct assessment of articular cartilage and underlying subchondral bone reveals a progressive gene expression change in human osteoarthritic knees. *Osteoarthritis Cartilage*. 2012; 21:450–61.10.1016/j.joca.2012.11.016. [PubMed: 23220557]
2. Derwin KA, Baker AR, Iannotti JP, McCarron JA. Preclinical models for translating regenerative medicine therapies for rotator cuff repair. *Tissue Eng Part B Rev*. 2010; 16:21–30.10.1089/ten.TEB.2009.0209. [PubMed: 19663651]
3. Gotoh M, Hamada K, Yamakawa H, Nakamura M, Yamazaki H, Ueyama Y, et al. Perforation of rotator cuff increases interleukin 1beta production in the synovium of glenohumeral joint in rotator cuff diseases. *J Rheumatol*. 2000; 27:2886–92. [PubMed: 11128681]
4. Hsu HC, Luo ZP, Stone JJ, Huang TH, An KN. Correlation between rotator cuff tear and glenohumeral degeneration. *Acta Orthop Scand*. 2003; 74:89–94.10.1080/00016470310013725. [PubMed: 12635800]
5. Lehmann LJ, Schollmeyer A, Stoeve J, Scharf HP. Biochemical analysis of the synovial fluid of the shoulder joint in patients with and without rotator cuff tears. *Z Orthop Unfall*. 2010; 148:90–4.10.1055/s-0029-1186112. [PubMed: 20135595]
6. Link TM, Li X. Bone marrow changes in osteoarthritis. *Semin Musculoskelet Radiol*. 2011; 15:238–46.10.1055/s-0031-1278423. [PubMed: 21644197]
7. Liu X, Manzano G, Kim HT, Feeley BT. A rat model of massive rotator cuff tears. *Journal of orthopaedic research: official publication of the Orthopaedic Research Society*. 2011; 29:588–95.10.1002/jor.21266. [PubMed: 20949443]
8. Mankin HJ, Dorfman H, Lippiello L, Zarins A. Biochemical and metabolic abnormalities in articular cartilage from osteo-arthritic human hips. II. Correlation of morphology with biochemical and metabolic data. *J Bone Joint Surg Am*. 1971; 53:523–37. [PubMed: 5580011]
9. Neer CS 2nd, Craig EV, Fukuda H. Cuff-tear arthropathy. *J Bone Joint Surg Am*. 1983; 65:1232–44. [PubMed: 6654936]

10. Oh JH, Jun BJ, McGarry MH, Lee TQ. Does a critical rotator cuff tear stage exist?: a biomechanical study of rotator cuff tear progression in human cadaver shoulders. *J Bone Joint Surg Am.* 2011; 93:2100–9.10.2106/JBJS.J.00032. [PubMed: 22262382]
11. Osawa T, Shinozaki T, Takagishi K. Multivariate analysis of biochemical markers in synovial fluid from the shoulder joint for diagnosis of rotator cuff tears. *Rheumatol Int.* 2005; 25:436–41.10.1007/s00296-004-0509-2. [PubMed: 15378264]
12. Reuther KE, Sarver JJ, Schultz SM, Lee CS, Sehgal CM, Glaser DL, et al. Glenoid cartilage mechanical properties decrease after rotator cuff tears in a rat model. *Journal of orthopaedic research: official publication of the Orthopaedic Research Society.* 2012; 30:1435–9.10.1002/jor.22100. [PubMed: 22407524]
13. Roemhildt ML, Beynon BD, Gardner-Morse M, Anderson K, Badger GJ. Tissue modification of the lateral compartment of the tibio-femoral joint following in vivo varus loading in the rat. *J Biomech Eng.* 2012; 134:104501.10.1115/1.4007453 [PubMed: 23083201]
14. Rutgers M, van Pelt MJ, Dhert WJ, Creemers LB, Saris DB. Evaluation of histological scoring systems for tissue-engineered, repaired and osteoarthritic cartilage. *Osteoarthritis Cartilage.* 2010; 18:12–23.10.1016/j.joca.2009.08.009. [PubMed: 19747584]
15. Soslowsky LJ, Carpenter JE, DeBano CM, Banerji I, Moalli MR. Development and use of an animal model for investigations on rotator cuff disease. *J Shoulder Elbow Surg.* 1996; 5:383–92. [PubMed: 8933461]
16. Tajana MS, Murena L, Valli F, Passi A, Grassi FA. Correlations between biochemical markers in the synovial fluid and severity of rotator cuff disease. *Chir Organi Mov.* 2009; 93(Suppl 1):S41–8.10.1007/s12306-009-0004-8 [PubMed: 19711169]
17. Yoshihara Y, Hamada K, Nakajima T, Fujikawa K, Fukuda H. Biochemical markers in the synovial fluid of glenohumeral joints from patients with rotator cuff tear. *Journal of orthopaedic research: official publication of the Orthopaedic Research Society.* 2001; 19:573–9.10.1016/S0736-0266(00)00063-2. [PubMed: 11518264]

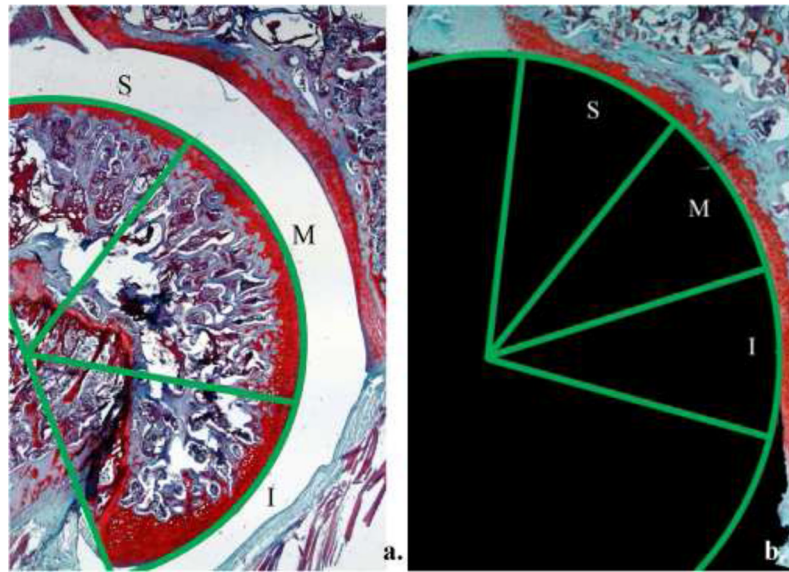


Figure 1. The humerus was divided into three discrete regions for analysis by dividing the arc of the humerus into thirds (a). An identical method was used for regional analysis of the glenoid (b). S = superior, M = middle, and I = inferior.

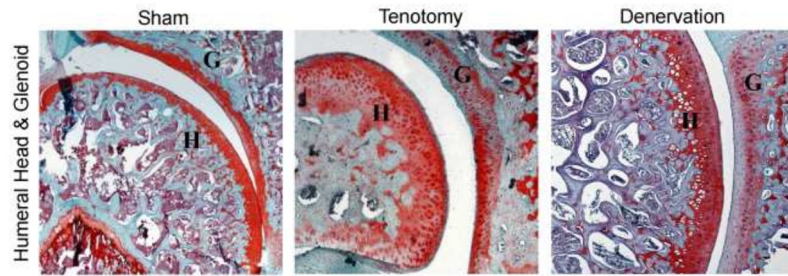


Figure 2. Coronal sections of the the glenohumeral joint at 5x. Note the structural irregularities, hypercellularity, loss of safranin-O staining, and loss of tidemark integrity in both surgical samples as compared to sham side (control).

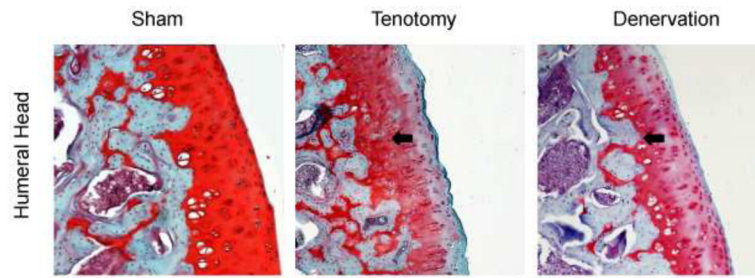


Figure 3. Coronal sections of the inferior region of the humeral head at 10x. Note the structural irregularities, hypercellularity, loss of safranin-O staining, and loss of tidemark integrity in both surgical samples as compared to sham side (control). Arrows denote recessed tidemark.

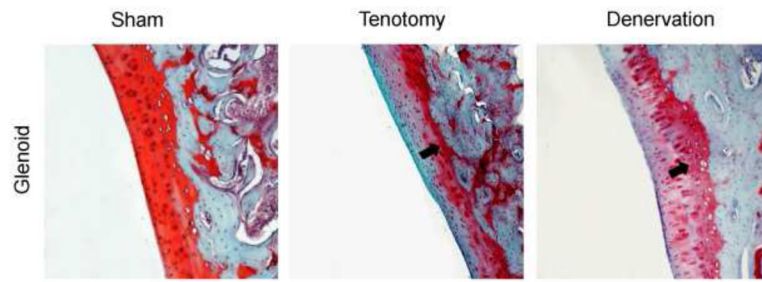


Figure 4. Coronal sections of the inferior region of the glenoid at 10x. Note the structural irregularities, hypercellularity, loss of safranin-O staining, and loss of tidemark integrity in both surgical samples as compared to sham side (control). Arrows denote recessed tidemark.

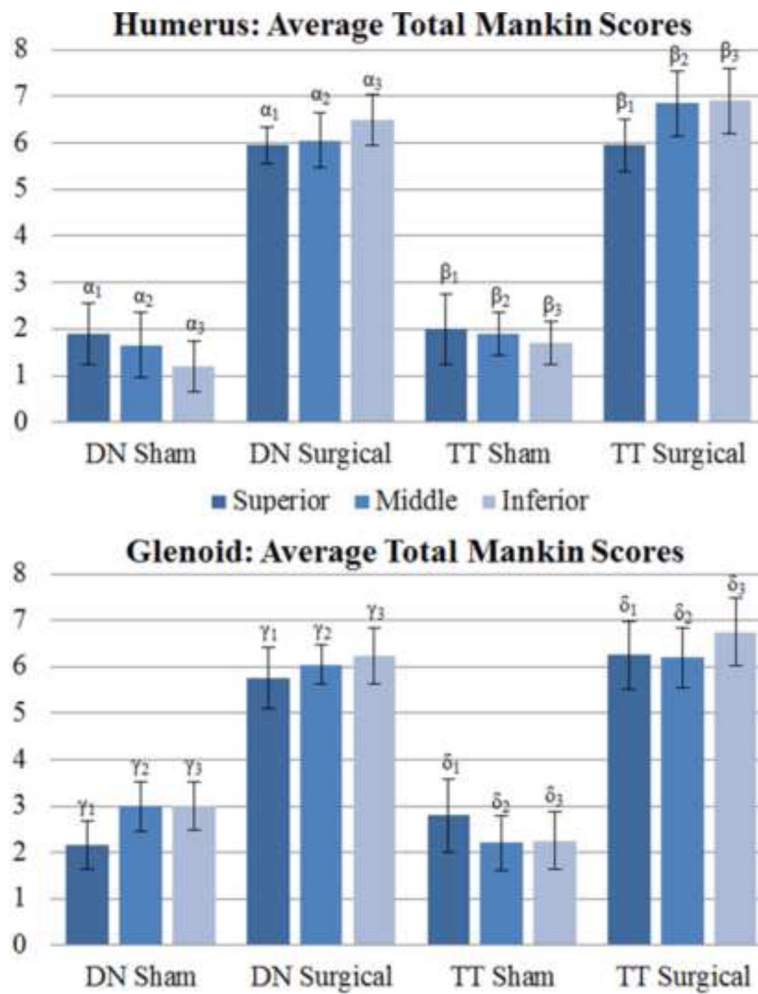


Figure 5. Average total Mankin scores by cartilage type, region, and group. p-values: $\alpha_1=0.01$, $\alpha_2<0.01$, $\alpha_3=0.01$, $\beta_1=0.01$, $\beta_2=0.01$, $\beta_3=0.01$, $\gamma_1=0.01$, $\gamma_2=0.01$, $\gamma_3=0.01$, $\delta_1=0.01$, $\delta_2=0.01$, $\delta_3=0.01$.

Table I

The Mankin scoring system was utilized to quantify cartilage quality using the four parameters of structure, cellularity, safranin-O staining, and tidemark integrity.

Mankin Scoring System	Grade
I. Structure	
a. Normal	0
b. Surface irregularities	1
c. Pannus and surface irregularities	2
d. Clefts to transitional zone	3
e. Clefts to radial zone	4
f. Clefts to calcified zone	5
g. Complete disorganization	6
II. Cellularity	
a. Normal	0
b. Diffuse hypercellularity	1
c. Cloning	2
d. Hypocellularity	3
III. Safranin-O staining	
a. Normal	0
b. Slight reduction	1
c. Moderate reduction	2
d. Severe reduction	3
e. No dye noted	4
IV. Tidemark integrity	
a. Intact	0
b. Crossed by blood vessels	1

Table II

Average total scores for humeral cartilage; both subscores and total scores are shown.

		Mankin Scores for Humeral Cartilage			
		Tendon Transection		Denervation	
		Sham	Surgical	Sham	Surgical
Superior	Str	0.50	1.20	0.50	1.40
	Cell	0.50	1.20	0.50	1.00
	Saf	0.30	2.55	0.70	2.75
	Tide	0.70	1.00	0.70	0.80
Total		2.00±0.52	5.95±0.66*	1.90±0.65	5.95±0.39*
Middle	Str	0.60	1.20	0.60	1.30
	Cell	0.50	1.45	0.50	1.20
	Saf	0.30	3.20	0.40	2.85
	Tide	0.50	1.00	0.15	0.70
Total		1.90±0.54	6.85±0.42*	1.65±0.70	6.05±0.59*
Inferior	Str	0.5	1.20	0.40	1.40
	Cell	0.40	1.75	0.30	1.50
	Saf	0.30	3.05	0.40	2.90
	Tide	0.50	0.90	0.10	0.70
Total		1.70±0.52	6.90±0.61*	1.20±0.55	6.50±0.55*

Str = structure, Cell = cellularity, Saf = safranin-O staining, and Tide = tidemark integrity, all in accordance with the Mankin scoring system. Significance of $p < 0.05$ versus controls indicated by *.

Table III

Age total scores for glenoid cartilage; both subscores and total scores are shown.

	Mankin Scores for Glenoid Cartilage				
	Tendon Transection		Denervation		
	Sham	Surgical	Sham	Surgical	
Superior	Str	0.50	0.80	0.10	0.90
	Cell	0.50	1.40	0.60	1.00
	Saf	1.10	3.15	1.25	2.85
	Tide	0.70	0.90	0.20	1.00
	Total	2.80±0.78	6.25±0.72*	2.15±0.76	5.75±0.55*
Middle	Str	0.40	0.90	0.00	1.00
	Cell	0.40	1.40	1.00	1.20
	Saf	0.60	3.00	1.60	2.95
	Tide	0.80	0.90	0.40	0.90
	Total	2.20±0.59	6.20±0.64*	3.00±0.47	6.05±0.70*
Inferior	Str	0.40	1.10	0.00	0.70
	Cell	0.40	1.60	0.90	1.40
	Saf	0.65	3.15	1.50	3.24
	Tide	0.80	0.90	0.60	0.90
	Total	2.25±0.63	6.75±0.74*	1.20±0.55	6.24±0.70*

Str = structure, Cell = cellularity, Saf = safranin-O staining, and Tide = tidemark integrity, all in accordance with the Mankin scoring system. Significance of $p < 0.05$ versus controls indicated by *.